TITLE PAGE

- Food Science of Animal Resources -

Upload this completed form to website with submission

ARTICLE INFORMATION	Fill in information in each box below
Article Type	Research article
Article Title	Investigation of Immunostimulatory Effects of Heat-treated *Lactiplantibacillus plantarum* LM1004 and its Underlying Molecular Mechanisms
Running Title (within 10 words)	Immunostimulatory Effects of Heat-treated *Lactiplantibacillus plantarum* LM1004
Author	Won-Young Bae[1,*], Woo-Hyun Jung[1], So Lim Shin[1], Seulgi Kwon[1], Minn Sohn[1], and Tae-Rahk Kim[1]
Affiliation	1 Microbiome R&D Center, Lactomason
Special remarks – if authors have additional information to inform the editorial office	I wish to submit for special issue “New concept of probiotics for human and animal health”
ORCID (All authors must have ORCID) https://orcid.org	Won-Young Bae (https://orcid.org/ 0000-0002-6615-2547) Woo-Hyun Jung (https://orcid.org/ 0000-0003-2474-1973) So Lim Shin (https://orcid.org/ 0000-0002-1683-4638) Seulgi Kwon (https://orcid.org/ 0000-0003-3134-8790) Minn Sohn (https://orcid.org/ 0000-0001-6278-1795) Tae-Rahk Kim (https://orcid.org/ 0000-0002-8066-1161)
Conflicts of interest List any present or potential conflict s of interest for all authors. (This field may be published.)	The authors declare no potential conflict of interest.
Acknowledgements State funding sources (grants, funding sources, equipment, and supplies). Include name and number of grant if available. (This field may be published.)	This research was supported by the Jinju Bioindustry Foundation
Author contributions (This field may be published.)	Conceptualization: Shin SL, Sohn M, Kim TR. Data curation: Jung WH, Shin SL. Formal analysis: Bae WY. Methodology: Bae WY. Software: Bae WY, Shin SL, Kwon S. Validation: Shin SL, Kwon S. Investigation: Bae WY, Jung WH. Writing - original draft: Bae WY. Writing - review & editing: Bae WY, Jung WH, Shin SL, Kwon S, Sohn M, Kim TR
Ethics approval (IRB/IACUC) (This field may be published.)	This article does not require IRB/IACUC approval because there are no human and animal participants.

CORRESPONDING AUTHOR CONTACT INFORMATION

For the <u>corresponding</u> author (responsible for correspondence, proofreading, and reprints)	**Fill in information in each box below**
First name, middle initial, last name	Won-Young Bae
Email address – this is where your proofs will be sent	wybae@lactomason.com
Secondary Email address	
Postal address	Microbiome R&D Center, Lactomason, Seoul 06620, Korea
Cell phone number	+82 10-2885-3101

ACCEPTED

Office phone number	+82 2-2677-0073
Fax number	+82 2-2677-0074

7
8

ACCEPTED

Authors and affiliation information should be listed on a separate Title Page.

Abstract (within 250 words)

Postbiotics are defined as probiotics inactivated by heat, ultraviolet radiation, sonication, and other physical or chemical stresses. Postbiotics are more stable than probiotics, and these properties are advantageous for food additives and pharmacological agents. This study investigated the immunostimulatory effects of heat-treated *Lactiplantibacillus plantarum* LM1004 (HT-LM1004). Cellular fatty acid composition of *L. plantarum* LM1004 isolated form kimchi was analyzed by GC/MSD system. The nitric oxide (NO) content was estimated using Griess reagent. Immunostimulatory cytokines were evaluated using enzyme-linked immunosorbent assay (ELISA). Relative protein expressions were evaluated by western blotting. Phagocytosis was measured using enzyme-labelled *Escherichia coli* particles. *L. plantarum* LM1004 showed 7 kinds of cellular fatty acids including palmitic acid (C16:0). The HT-LM1004 induced release of NO and upregulated the inducible nitric oxide synthase in RAW 264.7 macrophage cells. Tumor necrosis factor-α (TNF-α) and interleukin-6 (IL-6) levels were also increased compared to control (non-treated macrophages). Furthermore, HT-LM1004 modulated mitogen-activated protein kinase (MAPK) subfamilies including p38 MAPK, ERK1/2, and JNK. Therefore, these immunostimulatory effects were attributed to the production of transcriptional factors, such as nuclear factor kappa B (NF-κB) and the activator protein 1 family (AP-1). However, HT-LM1004 did not showed significant phagocytosis of RAW 264.7 macrophage cells. Overall, HT-LM1004 stimulated MAPK/AP-1 and NF-κB expression, resulting in the release of NO and cytokines. These results will contribute to the development of diverse types of food and pharmacological products for immunostimulatory agents with postbiotics.

Keywords *Lactiplantibacillus plantarum*, postbiotics, immunostimulatory effect, nuclear factor kappa B

Introduction

Lactic acid bacteria (LAB), regarded as useful probiotics, play a crucial role in fortifying the intestinal barrier against food-borne pathogenic bacteria (Kao et al., 2020; Levit et al., 2019) and modulating intestinal microbiota and immune systems (Levit et al., 2019). LAB have been consumed in various types of foods, including dairy products (Oshiro et al., 2021; Parvarei et al., 2021), fermented fruits and vegetables (Lorn et al., 2021; Oshiro et al., 2021), sourdough (Oshiro et al., 2021), and meat products (Parlindungan et al., 2021). Currently, LAB are used as pharmaceutical agents and not limited to probiotics (Barros et al., 2020). Postbiotics, which are inactivated probiotics (Barros et al., 2020; Parvarei et al., 2021) and their metabolites, have been investigated in a broad spectrum of food and pharmaceutical industries (Barros et al., 2020).

Innate immune system operates as the first-line defense in the host (Lee et al., 2020). Myeloid cells (macrophages, monocytes, and neutrophils) are critical components of innate immunity (Mantovani and Netea, 2020). Myeloid cells recognize pathogen-associated molecular patterns (PAMPs) from infectious microbes and danger-associated molecular patterns (DAMPs) from injured tissues caused by Toll-like receptors (TLRs), retinoic acid-inducible gene I (RGI-I)-like receptors (RLRs), nucleotide-binding oligomerization domain (NOD)-like receptor family proteins (NLRs), and absent in melanoma 2 (AIM2), a family of pattern-recognition receptors (PRRs) (Lee et al., 2020). Innate immune system activates macrophages and immediately counteracts to pathogens to provide host defenses against various types of invaders (Geng et al., 2018; Jeong et al., 2019; Lee et al., 2020; Leopold Wager and Wormley, 2014; Liu et al., 2019; Mantovani

and Netea, 2020; Netea et al., 2020; Um et al., 2020). Unlike these rapid reactions, the trained immune system involves reprogramming of innate immune cells awakened by exogenous or endogenous stimulations (Netea et al., 2020). For example, monocytes that were first treated with β-glucan lost stimulus within 24 h, and the second challenge by lipopolysaccharides (LPS) showed a burst of tumor necrosis factor-α (TNF-α) and interleukin-6 (IL-6) (Bauer et al., 2018). These well-trained cells undergo epigenetic modifications and have long-term memory effects (Bauer et al., 2018; Netea et al., 2020).

Lactiplantibacillus plantarum is a facultative heterofermentative *Lactobacillus* species (Liu et al., 2018). The European Food Safety Authority (EFSA) has acknowledged *L. plantarum* as a Qualified Presumption of Safety (QPS) and has continuously updated its strains since 2007 (Andreoletti et al., 2008; Liu et al., 2018). *L. plantarum* has been used not only for starter culture in the food industry (Le and Yang, 2018; Liu et al., 2018) but also in pharmacological research owing to its bio-functionalities (Le and Yang, 2018).

The aim of this study is investigation of immunostimulatory effects of heat-treated *L. plantarum* LM1004 (HT-LM1004). Other studies have been focused on the immunostimulatory effects of probiotics and their metabolites, such as exopolysaccharides, whereas heat-treated probiotics are not of interest. It had been known that heat treatment disrupts the bacterial cell wall and induces release of nucleic acid, peptidoglycan, and teichoic acids, resulting in modulating immune responses by these strain specific bacterial components (Piqué et al., 2019). Our previous study, micronized and heat-treated *L. plantarum* (MHT-LM1004) and HT-LM1004 showed increase of NK cell activity and relative cytokine production in immune-suppressed mice (Jung et al., 2019). However, molecular level mechanisms of immunostimulatory effect of HT-LM1004 were not fully understood. In addition, MHT-LM1004 is defined as similar material due to manufacturing methods and is not suitable for industrial production.

Therefore, the immunostimulatory effects of HT-LM1004 via the mitogen-activated protein kinase (MAPK)/Activator protein 1 family (AP-1)/Nuclear factor kappa B (NF-κB) pathway were investigated in this study.

Materials and Methods

Reagents and chemicals

Lipopolysaccharides from *Escherichia coli* O111:B4 (LPS) and ammonium pyrrolidine dithiocarbamate (APDC) were purchased from Sigma-Aldrich (St. Louis, MO, USA). Thiazolyl Blue tetrazolium bromide (MTT) was obtained from Alfa Aesar (Haverhill, MA, USA). Antibodies against COX-2, phospho-p38 MAPK, p38 MAPK, phospho-ERK1/2, ERK1/2, phospho-JNK, JNK, c-Fos, c-Jun, phospho-IκBα, IκBα, phospho-p65 NF-κB, p65 NF-κB, phospho-AMPK, AMPK, phospho-ACC, ACC, and GAPDH were obtained from Cell Signaling Technology (Danvers, MA, USA). The anti-iNOS antibody was obtained from GeneTex (Irvine, CA, USA).

Isolation of *Lactiplantibacillus plantarum* LM1004 and complete genome sequencing

Lactiplantibacillus plantarum LM1004 was isolated from kimchi, Korean traditional fermented food. In brief, 25 g of kimchi was homogenized in 225 mL of phosphate buffered saline (PBS) using a stomacher. After homogenization, sample was diluted in peptone water (0.1%, w/v) and spread on de Man-Rogosa-Sharpe (MRS) agar (for *Lactobacillus*) (BD, Franklin Lakes, NJ, USA), M17 agar (for lactic *Streptococcus* and *Lactococcus*) (MBcell, Seoul, South Korea), and *Bifidobacterium* selective agar (*Bifidobacterium* spp.) (MBcell). The spread agar plates were incubated at 37°C for 48 h. After 48 h, colonies isolated from MRS agar were spread on Bromocresol purple (BCP)

agar and yellow colonies on BCP agar further purified in newly prepared MRS agar until single colony. Single and pure colony was enriched in MRS broth for gram-staining and catalase reaction. The isolate was identified gram-positive and catalase-negative strain with rod-type shape. Isolated strain was named LM1004 and identified by 16S rRNA sequencing as *L. plantarum*. *L. plantarum* LM1004 was stored in MRS containing with 20% glycerol at –80°C until use (Ngamsomchat et al., 2022).

For analysis of complete genome sequencing, genomic DNA (gDNA) of *L. plantarum* LM1004 was extracted by TaKaRa MiniBEST Bacteria Genomic DNA Extraction Kit (Takara Bio, Kusatsu, Japan). The DNA sequencing library was constructed using single molecular real-time (SMRT) sequencing technology (Pacific Biosciences, Menlo Park, CA, USA). *De novo* assembly was performed using Celera Assembler in hierarchical genome assembly process (HGAP) (Macrogen, Seoul, South Korea).

Preparation of heat-treated *Lactiplantibacillus plantarum* LM1004

HT-LM1004 was obtained from the Department of Production, Lactomason (Gyeongsangnam-do, South Korea). The cell numbers and morphology were constantly managed by the Quality Management Team (Lactomason). Lyophilized heat-treated cells were assigned the product number 11NTF8 and stored at -20 ℃ until use.

Cellular fatty acid composition of heat-treated *Lactiplantibacillus plantarum* LM1004

Extraction of cellular fatty acid from HT-LM1004 was performed by Bligh and Dyer method with modification (Cheng et al., 2022). Briefly, 200 μL of chloroform/methanol solution (2:1, v/v) and 300 μL of 0.6 M hydrochloric acid solution (in methanol) were added in 20 mg of HT-LM1004. The mixture was shaken for 2 min vigorously and heated

at 85℃ during 60 min. The extracted lipids were cooled at 25℃ for 20 min. Fatty acid methyl esters (FAME) were more extracted by *n*-hexane for 60 to 120 min. The FAME extracted layer (*n*-hexane layer) was transferred into clear vial and stored at -20℃ until analysis.

Cellular fatty acid analysis was performed by GC/MSD. The GC/MSD system was composed of Agilent 8890 gas chromatography system coupled with a 5977B mass selective detector (MSD) and 7693A automated liquid sampler (Agilent, Santa Clara, CA, USA). An Agilent J&W DB-FastFAME capillary column packed with cyanopropyl (30 m × 0.25 mm, 0.25 μm) was employed. Injection port temperature was 250℃ in constant flow and 1 μL of sample was injected using the spilt mode of 20:1. Ultrapure helium gas was used as carrier gas with a flow rate of 1mL/min. The initial oven temperature was retained at 60℃ for 1 min, raised from 60℃ to 165℃ at a rate of 60℃/min, held 1 min at 165℃, raised form 165℃ to 230℃ at a rate of 5℃/min, and kept for 3 min. The temperature of ion source and transfer line was 230℃, and 250℃, respectively. The mass spectra were obtained on an electron ionization (EI) at 70 eV and recorded *m/z* 40-550 of mass range. Methyl undecanoate was used as internal standard (Liu et al., 2022).

Cell culture and treatment

The murine macrophage cells, RAW 264.7 cell lines, were obtained from the Korean Cell Line Bank (KCLB, Seoul, South Korea). The cells were maintained in Dulbecco's modified Eagle's medium (DMEM) supplemented with 10% fetal bovine serum (FBS) and 1% penicillin-streptomycin solution at 37℃ in a humidified atmosphere containing 5% CO_2. When the cells were grown to 80% confluence, they were gently harvested using a scraper. Harvested cells were seeded in various well plates and incubated for 24 h. After incubation, cells were treated with LPS (10 ng/mL) or HT-LM1004 to measure

159 immunostimulatory and phagocytic effects (Liu et al., 2019). Cells were pre-treated with
160 APDC, an NF-κB inhibitor, for 1 h before treatment with LPS or HT-LM1004.
161
162 **Cell viability**
163 Macrophage cells were seeded in a 96-well microplate (1×10^5 cells/well) and incubated
164 for 24 h. After incubation, each well was treated with LPS or HT-LM1004 (1×10^7,
165 2.5×10^7, 5×10^7, and 1×10^8 cells/mL) and further incubated for 24 h. The incubated cells
166 were washed with PBS twice times and fresh DMEM including 0.5 mg/mL of MTT was
167 used to replace any lost medium (Um et al., 2020). The absorbance of MTT formazan
168 which viable cell converted was evaluated at 570 nm using a microplate reader
169 (SpectraMax iD3, Molecular Devices, San Jose, CA, USA). Cell viability was calculated
170 as follows:
171 $$\text{Cell viability (\%)} = \frac{A_{sample}}{A_{control}} \times 100$$
172 where A_{sample} is the absorbance of LPS or HT-LM1004 treated cells and $A_{control}$ is the
173 absorbance of non-treated cells (negative control).
174
175 **Nitric oxide production**
176 The nitric oxide (NO) content was measured using Griess reagent (Geng et al., 2018).
177 Briefly, RAW 264.7 macrophage cells (1×10^5 cells/well) were treated with LPS (positive
178 control) or HT-LM1004 for 24 h. After 24 h, cell-free supernatants were collected, and
179 added Griess reagent (Promega, Madison, WI, USA) for measuring NO contents
180 according to the manufacturer's guidelines.
181
182 **Cytokine production**
183 The release of immunostimulatory cytokines (TNF-α and IL-6) was measured using an

enzyme-linked immunosorbent assay (ELISA) (Bo et al., 2019; Liu et al., 2019). Cell culture and sample treatments were prepared as described in cell culture and treatment. Cell-free supernatants were collected by centrifugation at 1,000 ×g for 20 min at 4℃. All immunostimulatory cytokines were analyzed according to the manufacturer's guidelines (Invitrogen, Waltham, MA, USA).

In vitro phagocytosis

The phagocytic effect of HT-LM1004 treated RAW 264.7 macrophage cells was evaluated using enzyme-labeled *Escherichia coli* particles (CytoSelect™ 96-Well Phagocytosis Assay, Cell Biolabs, San Diego, CA, USA) (Jeong et al., 2019). Relative phagocytic effects were measured by enzyme-substrate reactions, according to the manufacturer's guidelines.

Western blot analysis

The HT-LM1004 treated RAW 264.7 macrophage cells were lysed by RIPA lysis buffer (containing 50 mM Tris-HCl, 150 mM NaCl, 1% Triton-X, 1% sodium deoxycholate, 0.1% SDS and 2 mM EDTA) with protease and phosphatase inhibitor cocktail (Thermo Fisher Scientific, Waltham, MA, USA). The lysed cells were centrifuged at 13,000 ×g for 20 min at 4℃. The supernatants were collected, and protein content was measured using the Pierce™ BCA Protein Assay Kit (Thermo Fisher Scientific). The extracted proteins were stored at 4℃ until further use.

Proteins were separated by capillary western blot analysis (Khan et al., 2021) or sodium dodecyl sulfate-polyacrylamide gel electrophoresis (SDS-PAGE). For capillary western blotting, proteins were diluted to 0.8 mg/mL and separated by a 12-230 kDa capillary cartridge (ProteinSimple, San Jose, CA, USA) according to the manufacturer's guidelines.

Protein separation and immunodetection were conducted using JESS, an automated western blotting system (ProteinSimple).

For SDS-PAGE, proteins (30 μg) were separated to 8 or 10% of SDS-PAGE gel and transferred onto polyvinylidene fluoride membranes. Membranes were blocked with 3.75% skim milk for 1 h, followed by incubation with primary antibodies at 4℃ for 24 to 48 h. After incubation, the membranes were washed with Tris-buffered saline containing Tween 20 (TBS-T) and incubated with secondary antibodies at 25℃ for 2 h. The blots were visualized using ECL detection reagent (Advansta, San Jose, CA, USA). The intensity of the bands was analyzed using ImageJ software.

Statistical analysis

Statistical analyses were performed using SPSS Statistics version 18 software (IBM, Armonk, NY, USA). HT-LM1004 treated groups were compared with the negative control (non-treated group). The mean values were analyzed using a t-test at $p<0.05$.

Results

Complete genome sequencing of *L. plantarum* LM1004 and cellular fatty acid composition of HT-LM1004

The whole genome characteristics of *L. plantarum* LM1004 are shown in Fig. 1A. The size of entire gene sequence of *L. plantarum* LM 1004 was 3,198,690 bp, single and circular chromosome with 44.59% of GC content. A total of 3001 protein-coding sequences (CDS) were identified in *L. plantarum* LM1004. The chromosome include 16 rRNA and 68 tRNA. The complete genome sequence of *L. plantarum* LM1004 has been deposited in the National Center for Biotechnology Information GenBank database under the accession number CP025988.

Cellular fatty acid composition of HT-LM1004 are shown in Fig. 1B and 1C. Total 7 kinds of fatty acid were observed in HT-LM1004. Lactobacillic acid (cycC19:0) and palmitic acid (C16:0) were investigated most abundant cellular fatty acid in HT-LM1004. The proportion of saturated fatty acid (SFA), unsaturated fatty acid (USFA) and cyclic fatty acid (CFA) in HT-LM1004 were measured 41.42%, 20.03, and 38.55%, respectively.

NO production and inducible nitric oxide synthase (iNOS) expression

Prior to measuring the immunostimulatory effects of HT-LM1004, cell viability was investigated using MTT formazan. Cytotoxicity was not shown in HT-LM1004 or LPS treated (positive control) macrophage cells (Fig. 2A). The NO content and iNOS expression are shown in Fig. 2B and 2C. The HT-LM1004 (1×10^7, 2.5×10^7, 5×10^7, and 1×10^8 cells/mL) treated RAW 264.7 macrophage cells released 3.05, 7.55, 12.55, and 16.32 μM of NO, respectively ($p<0.01$). The relative expression of iNOS increased 6.59-, 14.24-, 17.14-, and 19.86-fold compared to non-treated RAW 264.7 macrophages (negative control) ($p<0.01$).

Immunostimulatory cytokines and COX-2 expression

The release of immunostimulatory cytokines (TNF-α and IL-6) and relative protein expression of COX-2 are shown in Fig. 3. HT-LM1004 increased TNF-α secretion from 205.52 (negative control) to 1530.11, 1925.27, 3445.44, and 3906.01 pg/mL ($p<0.01$). In addition, HT-LM1004 treated RAW 264.7 macrophages released 254.36, 302.66, 394.29, and 651.93 pg/mL of the immunostimulatory cytokine IL-6 ($p<0.01$). The relative protein ex-pression of COX-2 was up-regulated in HT-LM1004 treated RAW 264.7 macrophage cells. COX-2 expression increased to 25.25-fold at 1×10^8 cells/mL of HT-LM1004 treated RAW 264.7 macrophage cells ($p<0.001$) (Fig. 3C).

Modulation of MAPK and transcriptional factor

Fig. 4 and 5 present changes in MAPK and transcription factor in HT-LM1004 treated RAW 264.7 macrophage cells. HT-LM1004 treated RAW 264.7 macrophage cells were used to investigate the phosphorylation of MAPK sub-families (p38, ERK1/2, and JNK). Briefly, phosphorylation of p38 MAPK, ERK1/2, and JNK increased to 4.96-, 5.52-, and 2.98-fold at 1×10^8 cells/mL of HT-LM1004 treated macrophage cells ($p<0.05$). Moreover, phosphorylation of IκBα and activation of NF-κB p65 translocation were observed in HT-LM1004 treated cells (Fig. 5) ($p<0.01$). Other transcription factors (c-Fos and c-Jun) also increased protein expression ($p<0.05$).

Modulation of NO level and iNOS expression in pharmacological inhibitor treated cells

APDC, a pharmacological NF-κB inhibitor, prevents iNOS expression and NO production (Dong et al., 2015). In the current study, the immunostimulatory effects of HT-LM1004 were investigated by the upregulation of iNOS and the release of NO in APDC-treated RAW 264.7 macrophage cells. The APDC-treated cells inhibited the release of NO (3.81 μM) though HT-LM1004 treated cells produced 4.46 and 7.31 μM of NO at 5×10^7 and 1×10^8 cells/mL, respectively ($p<0.01$). The APDC and HT-LM1004 co-treated cells also showed an over-expressed iNOS level comparing to non-treated RAW 264.7 macrophage cells ($p<0.001$) (Fig. 6).

Phagocytosis

The phagocytic effect of HT-LM1004 treated cells is shown in Fig. 7. The 1×10^7 cells/mL of HT-LM1004 treatment increased phagocytosis of macrophage cells

(123.18%), but no significant differences were detected. Phosphorylation of AMPK and ACC did not significantly change in the HT-LM1004 treated macrophages.

Discussion

The interactions between LAB and the host immune system have not been clearly reported, but many researchers have suggested that PRRs recognize LAB cell wall-derived molecules as PAMPs (Ren et al., 2020). Lipoteichoic acid (LTA), the most representative cell wall-derived PAMP in gram-positive bacteria, is an important ligand for innate immune responses (Friedrich et al., 2022; Jung et al., 2022; Kang et al., 2011; Ren et al., 2020). LTA is an amphiphilic molecule with both a hydrophilic polysaccharide moiety and a hydrophobic glycolipid region (Kang et al., 2011). In general, LTA interacts with TLR2, which is associated with myeloid differentiation primary response 88 (MyD88), interleukin-1 receptor (IL-1R)-associated kinases (IRAKs), and TNF receptor-associated factor 6 (TRAF6) (Jung et al., 2022). These TLR2-MyD88 dependent signaling pathways upregulate release of immunostimulatory cytokines and chemokines (Kang et al., 2011). The immunogenicity of LTA depends on its structural diversity in accordance with the genus and species levels (Friedrich et al., 2022). Ryu et al. (2009) reported that LTA isolated from three different gram-positive bacteria (*Staphylococcus aureus*, *Bacillus subtilis*, *L. plantarum*) showed relative differences in NF-κB translocation and TNF-α secretion. Moreover, Jung et al. (2022) reported differential immunostimulatory effects of LTA isolated from four different strains of *L. plantarum* and analyzed differences in glycolipid composition. Considering the immunogenicity of LTA, heat-treated LAB also showed immunomodulatory effects of LTA. In the current study, HT-LM1004 induced the release of immunostimulatory cytokines (TNF-α and IL-6) (Fig. 3) and translocation of NF-κB (Fig. 5). These results were also observed in other

heat-treated *L. plantarum* species (Choi et al., 2018; Jeong et al., 2019; Moon et al., 2019). In addition, Kim et al. (2018) reported that heat-treated LAB contributed immunomodulatory food additives and prolonged the shelf life.

NO is synthesized in various cells for neurotransmission, vascular function, host defense, and immune regulation (Xue et al., 2018). Nitric oxide synthases (NOS) are classified into three subtypes: neuronal nitric oxide synthase, endothelial nitric oxide synthase, and iNOS. In particular, iNOS is mainly expressed in immune-stimulated cells by cytokines and inflammatory molecules (PAMPs) such as LPS and LTA (Kang et al., 2011; Xue et al., 2018). NO plays a critical role in the regulation of M1 macrophage polarization. M1 macrophages are able to respond to pro-inflammatory responses and produce cytokines such as TNF-α, IL-6, and IL-12 for host defense (Yunna et al., 2020). Additionally, NO generated by iNOS expression in M1 macrophages directly defends against pathogens (Xue et al., 2018). HT-LM1004 induced release of NO levels and expressed iNOS in RAW 264.7 macrophage cells (Fig. 2). HT-LM1004 also affected the release of immunostimulatory cytokines (Fig. 3).

NF-κB signaling is crucial in physiological processes. NF-κB transcription factors are involved in cellular transformation and proliferation, apoptosis, angiogenesis, metastasis, and activation of the immune system (Aggarwal, 2004). In the immune system, the NF-κB transcription factor is involved in inflammatory responses to microbes and viruses by innate immune cells and the development of adaptive immune cells in secondary lymphoid organs (Dorrington and Fraser, 2019). IκBα degradation and phosphorylation activates the NF-κB transcription factor (p65) from the cytoplasm to the nucleus (Geng et al., 2018). The translocation of NF-κB mediates the transcription of immunostimulatory molecules and cytokines, including iNOS, COX-2, TNF-α, IL-2, IL-6, and IL-12 (Geng et al., 2018; Moon et al., 2019; Yang et al., 2019). TNF-α, IL-2, and

IL-12 contribute to the activation of natural killer (NK) cells, which play a crucial role in the host defense system against pathogens and transformed cells (Lauwerys et al., 2000; Moon et al., 2019). These cytokines promote cytotoxicity of NK cells and immunomodulatory effects of NK cells in the innate and adaptive immune systems (Lauwerys et al., 2000). In addition, Sharma and Das (2018) reported that IL-2 mediates the proliferation of NK cells.

The MAPK cascade promotes the transcription of transcriptional factors, such as NF-κB and activator protein 1 (AP-1) (Geng et al., 2018; Liu et al., 2019; Yang et al., 2019). AP-1 consists of four subfamilies: Jun, Fos, ATF-activating transcription factor protein families and musculoaponeurotic fibrosarcoma. AP-1 in immune system has been reported to play a role in Th differentiation, T-cell activation, and T-cell anergy (Atsaves et al., 2019). Activation of the MAPK pathway via a cascade of phosphorylation events on serine/threonine residues coordinates downstream of AP-1 and NF-κB (Atsaves et al., 2019; Geng et al., 2018). Thus, MAPK activation by HT-LM1004 plays a central role in the innate immune system.

Phagocytosis is occurred in three classes of phagocytic cells in immune system such as monocytes/macrophages, neutrophilic granulocytes and dendritic cells (Schumann, 2016). Macrophages act as scavenger of pathogens, dead cells, and debris. When macrophages engulf pathogens, phagosomes are fused with lysosomes which result in phagolysosomes and toxic peroxides for digesting the pathogens (Jeong et al., 2014; Schumann, 2016). Fatty acids can influence modulating of immune response of macrophages including phagocytosis and cytokine productions (Schumann, 2016). Calder et al. (1990) reported SFA such palmitic acid result in decrease of phagocytosis of macrophages. On the other hand, USFA increased phagocytosis of macrophages except oleic acid (C18:1). However, palmitic acid activate TLR-MyD88 dependent NF-κB activation and production of

immunostimulatory cytokines (Korbecki and Bajdak-Rusinek, 2019). In current study, the contents of SFA were measured 2-times higher than USFA in cellular fatty acid of HT-LM1004. Palmitic acid is a most abundant fatty acid except for lactobacillic acid which is CFA (Fig. 1B and 1C). The 1×10^7 cell/mL of HT-LM1004 treated cells showed highest phagocytosis effect (123.18%) while 1×10^8 cell/mL treated macrophage cells decreased to 116.69% (Fig. 7). However, palmitic acid derived from cellular membrane of HT-LM1004 induced immunostimulatory effects by activation of NF-κB (Fig. 5 and 6).

Conclusion

In the present study, the immunostimulatory potency of HT-LM1004 was investigated at various stages of innate immunity. HT-LM1004 stimulated the MAPK pathway and regulated transcription factors, such as AP-1 (c-Fos and c-Jun) and NF-κB p65. These transcription factors induce secretion of NO, TNF-α, and IL-6 to enhance the immune system. Heat-treated LAB lost their probiotic properties, but HT-LM1004 showed immunostimulatory effects as a postbiotic. These results suggest HT-LM1004 as an immunostimulatory agent, food additive, and therapeutic agent.

References

Aggarwal BB. 2004. Nuclear factor-κB: the enemy within. Cancer Cell 6:203–208.

Andreoletti O, Budka H, Buncic S, Colin P, Collins JD, De Koeijer A, Griffin J, Havelaar A, Hope J, Klein G, Kruse H, Magnino S, López AM, McLauchlin J, Nguyen-Thé C, Noeckler K, Noerrung B, Maradona MP, Roberts T, Vågsholm I, Vanopdenbosch E. 2008. The maintenance of the list of QPS microorganisms intentionally added to food or feed - Scientific Opinion of the Panel on Biological Hazards. EFSA J 6:923.

Atsaves V, Leventaki V, Rassidakis GZ, Claret FX. 2019. AP-1 transcription factors as regulators of immune responses in cancer. Cancers 11:1037.

Barros CP, Guimarães JT, Esmerino EA, Duarte MCK, Silva MC, Silva R, Ferreira BM, Sant'Ana AS, Freitas MQ, Cruz AG. 2020. Paraprobiotics and postbiotics: concepts and potential applications in dairy products. Curr Opin Food Sci 32:1–8.

Bauer M, Weis S, Netea MG, Wetzker R. 2018. Remembering pathogen dose: long-term adaptation in innate immunity. Trends Immunol 39:438–445.

Bo S, Dan M, Li W, Zhang P. 2019. Characterizations and immunostimulatory activities of a polysaccharide from *Arnebia euchroma* (Royle) Johnst. roots. Int J Biol Macromol 125:791–799.

Calder PC, Bond JA, Harvey DJ, Gordon S, Newsholme EA. 1990. Uptake and incorporation of saturated and unsaturated fatty acids into macrophage lipids and their effect upon macrophage adhesion and phagocytosis. Biochem J 269:807–814.

Cheng Z, Yan X, Wu J, Weng P, Wu Z. 2022. Effects of freeze drying in complex lyoprotectants on the survival, and membrane fatty acid composition of *Lactobacillus plantarum* L1 and *Lactobacillus fermentum* L2. Cryobiology 105:1–9.

Choi DW, Jung SY, Kang J, Nam YD, Lim SI, Kim KT, Shin HS. 2018. Immune-enhancing effect of nanometric *Lactobacillus plantarum* nF1 (nLp-nF1) in a mouse model of cyclophosphamide-induced immunosuppression. J Microbiol Biotechnol 28:218–226.

Dong Z, Su L, Esmaili S, Iseli TJ, Ramezani-Moghadam M, Hu L, Xu A, George J, Wang J. 2015. Adiponectin attenuates liver fibrosis by inducing nitric oxide production of hepatic stellate cells. J Mol Med 93:1327–1339.

Dorrington MG, Fraser IDC. 2019. NF-κB signaling in macrophages: dynamics, crosstalk, and signal integration. Front Immunol 10:705.

409 Friedrich AD, Leoni J, Paz ML, González Maglio DH. 2022. Lipoteichoic acid from
410 *Lacticaseibacillus rhamnosus* GG modulates dendritic cells and T cells in the gut.
411 Nutrients 14:723.
412 Geng L, Hu W, Liu Y, Wang J, Zhang Q. 2018. A heteropolysaccharide from *Saccharina*
413 *japonica* with immunomodulatory effect on RAW 264.7 cells. Carbohydr Polym
414 201:557–565.
415 Jeong M, Kim JH, Yang H, Kang SD, Song S, Lee D, Lee JS, Yoon Park JH, Byun S,
416 Lee KW. 2019. Heat-killed *Lactobacillus plantarum* KCTC 13314BP enhances
417 phagocytic activity and immunomodulatory effects via activation of MAPK and
418 STAT3 pathways. J Microbiol Biotechnol 29:1248–1254.
419 Jeong KM, Choi JI, Lee SH, Lee HJ, Son JK, Seo CS, Song SW, Kwak SH, Bae HB.
420 2014. Effect of sauchinone, a lignan from *Saururus chinensis*, on bacterial
421 phagocytosis by macrophages. Eur J Pahrmacol 728:176–182.
422 Jung BJ, Kim H, Chung DK. 2022. Differential immunostimulatory effects of lipoteichoic
423 acids isolated from four strains of *Lactiplantibacillus plantarum*. Appl Sci 12:954.
424 Jung IS, Jeon MG, Oh DS, Jung YJ, Kim HS, Bae D, Kim Y, Lee GE, Choi C, Hwang
425 YP. 2019. Micronized, heat-treated *Lactobacillus plantarum* LM1004 alleviates
426 cyclophosphamide-induced immune suppression. J Med Food 9:896–906.
427 Kang SS, Ryu YH, Baik JE, Yun CH, Lee K, Chung DK, Han SH. 2011. Lipoteichoic
428 acid from *Lactobacillus plantarum* induces nitric oxide production in the presence of
429 interferon-γ in murine macrophages. Mol Immunol 48:2170–2177.
430 Kao L, Liu TH, Tsai TY, Pan TM. 2020. Beneficial effects of the commercial lactic acid
431 bacteria product, Vigiis 101, on gastric mucosa and intestinal bacterial flora in rats. J
432 Microbiol Immunol Infect 53:266–273.
433 Khan HU, Aamir K, Jusuf PR, Sethi G, Sisinthy SP, Ghildyal R, Arya A. 2021. Lauric

434 acid ameliorates lipopolysaccharide (LPS)-induced liver inflammation by mediating
435 TLR4/MyD88 pathway in Sprague Dawley (SD) rats. Life Sci 265:118750.
436 Kim DH, Chung WC, Chun SH, Han JH, Song MJ, Lee KW. 2018. Enhancing the natural
437 killer cell activity and anti-influenza effect of heat-treated *Lactobacillus plantarum*
438 nF1-fortified yogurt in mice. J Dairy Sci 101:10675–10684.
439 Korbecki J, Bajdak-Rusinek K. 2019. The effect of palmitic acid on inflammatory
440 response in macrophages: an overview of molecular mechanisms. Inflamm Res
441 68:915–932.
442 Lauwerys BR, Garot N, Renauld JC, Houssiau FA. 2000. Cytokine production and killer
443 activity of NK/T-NK cells derived with IL-2, IL-15, or the combination of IL-12 and
444 IL-18. J Immunol 165:1847–1853.
445 Le B, Yang SH. 2018. Efficacy of *Lactobacillus plantarum* in prevention of inflammatory
446 bowel disease Toxicol Rep 5:314–317.
447 Lee S, Channappanavar R, Kanneganti TD. 2020. Coronaviruses: innate immunity,
448 inflammasome activation, inflammatory cell death, and cytokines. Trends Immunol
449 41:1083–1099.
450 Leopold Wager CM, Wormley FL. 2014. Classical versus alternative macrophage
451 activation: the Ying and the Yang in host defense against pulmonary fungal infections.
452 Mucosal Immunol 7:1023–1035.
453 Levit R, Savoy de Giori G, de Moreno de LeBlanc A, LeBlanc JG. 2019. Beneficial effect
454 of a mixture of vitamin-producing and immune-modulating lactic acid bacteria as
455 adjuvant for therapy in a recurrent mouse colitis model. Appl Microbiol Biotechnol
456 103:8937–8945.
457 Liu J, Wu C, Li X, Yan Q, Reaney MJT, Jiang Z. 2019. Xylose rich heteroglycan from
458 flaxseed gum mediates the immunostimulatory effects on macrophages via TLR2

459 activation. Carbohydr Polym 213:59–69.
460 Liu W, Pu X, Sun J, Shi X, Cheng W, Wang B. 2022. Effect of *Lactobacillus plantarum*
461 on functional characteristics and flavor profile of fermented walnut milk. LWT-Food
462 Sci Technol 160:113254.
463 Liu YW, Liong MT, Tsai YC. 2018. New perspectives of *Lactobacillus plantarum* as a
464 probiotic: the gut-heart-brain axis. J Microbiol 56:601–613.
465 Lorn D, Nguyen TKC, Ho PH, Tan R, Licandro H, Waché Y. 2021. Screening of lactic
466 acid bacteria for their potential use as aromatic starters in fermented vegetables Int J
467 Food Microbiol 350:109242.
468 Mantovani A, Netea MG. Trained innate immunity, epigenetics, and Covid-19. 2020. N
469 Engl J Med 383:1078–1080.
470 Moon PD, Lee JS, Kim HY, Han NR, Kang I, Kim HM, Jeong HJ. 2019. Heat-treated
471 *Lactobacillus plantarum* increases the immune responses through activation of natural
472 killer cells and macrophages on *in vivo* and *in vitro* models. J Med Microbiol 68:467–
473 474.
474 Netea MG, Domínguez-Andrés J, Barreiro LB, Chavakis T, Divangahi M, Fuchs E,
475 Joosten LAB, van der Meer JWM, Mhlanga MM, Mulder WJM, Riksen NP, Schlitzer
476 A, Schultze JL, Benn CS, Sun JC, Xavier RJ, Latz E. 2020. Defining trained immunity
477 and its role in health and disease. Nat Rev Immunol 20:375–388.
478 Ngamsomchat A, Kaewkod T, Konkit M, Tragoolpua Y, Bovonsombut S, Chitov T. 2022.
479 Characterisation of *Lactobacillus plantarum* of dairy-product origin for probiotic
480 chèvre cheese production. Foods 11:934.
481 Oshiro M, Zendo T, Nakayama J. 2021. Diversity and dynamics of sourdough lactic acid
482 bacteriota created by a slow food fermentation system. J Biosci Bioeng 131:333–340.
483 Parlindungan E, Lugli GA, Ventura M, van Sinderen D, Mahony J. 2021. Lactic acid

484 bacteria diversity and characterization of probiotic candidates in fermented meats.
485 Foods 10:1519.
486 Parvarei MM, Fazeli MR, Mortazavian AM, Nezhad SS, Mortazavi SA, Golabchifar AK,
487 Khorshidian N. 2021. Comparative effects of probiotic and paraprobiotic addition on
488 microbiological, biochemical and physical properties of yogurt. Food Res Int 131:334–
489 340.
490 Piqué N, Berlanga M, Miñana-Galbis D. 2019. Health benefits of heat-killed (tyndallized)
491 probiotics: an overview. Int J Mol Sci 20:2534.
492 Ren C, Cheng L, Sun Y, Zhang Q, de Haan BJ, Zhang H, Faas MM, de Vos P. 2020.
493 Lactic acid bacteria secrete toll like receptor 2 stimulating and macrophage
494 immunomodulating bioactive factors. J Funct Foods 66:103783.
495 Ryu YH, Baik JE, Yang JS, Kang SS, Im J, Yun CH, Kim DW, Lee K, Chung DK, Ju
496 HR, Han SH. 2009. Differential immunostimulatory effects of Gram-positive bacteria
497 due to their lipoteichoic acids. Int Immunopharmacol 9:127–133.
498 Schumann J. 2016. It is all about fluidity: fatty acids and macrophage phagocytosis. Eur
499 J Pharmacol 785:18–23.
500 Sharma R, Das A. 2018. IL-2 mediates NK cell proliferation but not hyperactivity.
501 Immunol Res 66:151–157.
502 Um Y, Eo HJ, Kim HJ, Kim K, Jeon KS, Jeong JB. 2020. Wild simulated ginseng
503 activates mouse macrophage, RAW264.7 cells through TRL2/4-dependent activation
504 of MAPK, NF-κB and PI3K/AKT pathways. J Ethnopharmacol 263:113218.
505 Xue Q, Yan Y, Zhang R, Xiong H. 2018. Regulation of iNOS on immune cells and its
506 role in diseases. Int J Mol Sci 19:3805.
507 Yang Y, Xing R, Liu S, Qin Y, Li K, Yu H, Li P. 2019. Immunostimulatory effects of
508 chitooligosaccharides on RAW 264.7 mouse macrophages via regulation of the MAPK

and PI3K/Akt signaling pathways. Mar Drugs 17:36.

Yunna C, Mengru H, Lei W, Weidong C. 2020. Macrophage M1/M2 polarization. Eur J Pharmacol 877:173090.

Tables and Figures

Tables and Figures can be placed in separate files.

ACCEPTED

Figure Legends

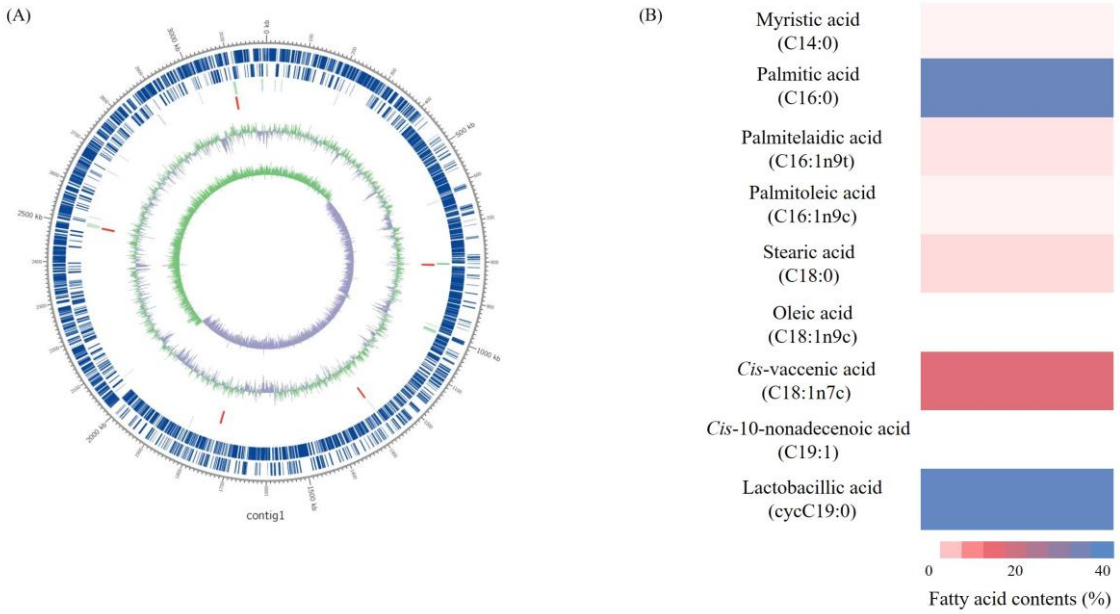

Fig. 1. Circular genome map of *Lactiplantibacillus* LM1004 and cellular membrane fatty acid analysis of heat-treated *Lactiplantibacillus plantarum* LM1004. (A) Circular genome map of *Lactiplantibacillus plantarum* LM1004. Each circle from outside to inside indicates protein-coding sequences (CDS) on forward strand, CDS on reverse strand, tRNA, rRNA, GC content, and GC skew. (B) cellular fatty acid composition of heat-treated *Lactiplantibacillus plantarum* LM1004.

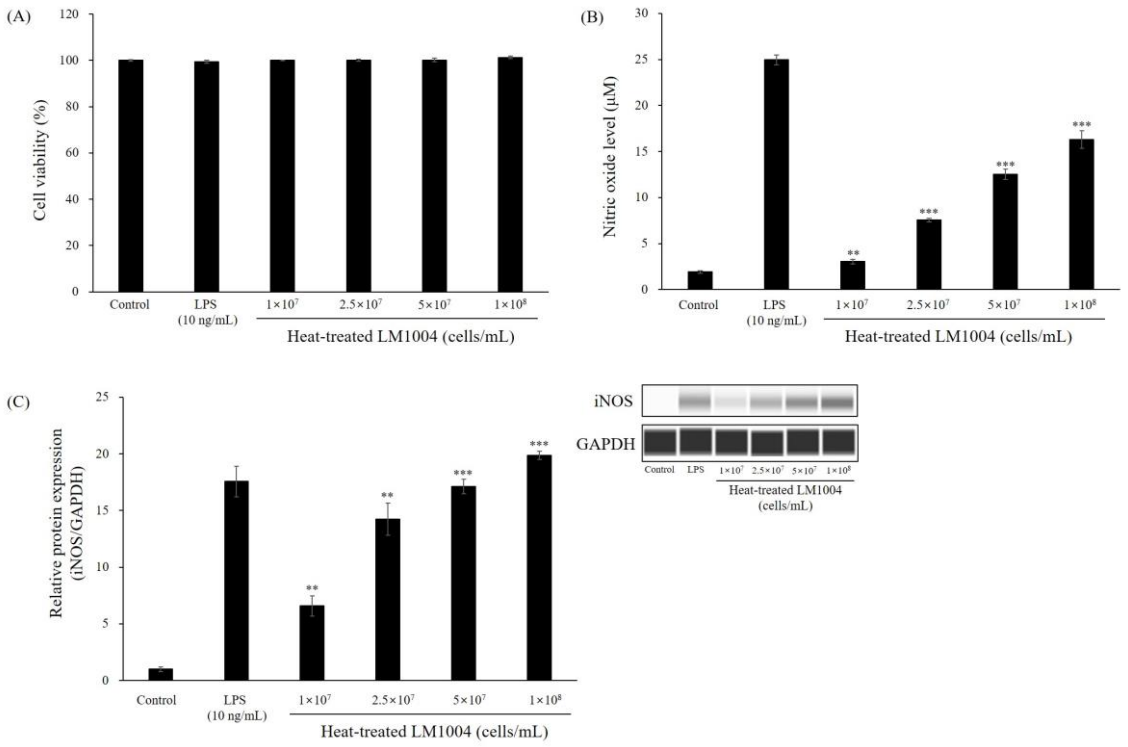

527

528 **Fig. 2. Nitric oxide production and relative protein expression of iNOS in**
529 **heat-treated *Lactiplantibacillus plantarum* LM1004 treated RAW 264.7**
530 **macrophage cells.** (A) cell viability of *Lactiplantibacillus plantarum* LM1004
531 treated RAW 264.7 macrophage cells, (B) release of nitric oxide in
532 *Lactiplantibacillus plantarum* LM1004 treated RAW 264.7 macrophage cells, (c)
533 relative protein expression in *Lactiplantibacillus plantarum* LM1004 treated RAW
534 macrophage 264.7 cells. Data are shown as the means±standard deviations of
535 three independent experiments. **p<0.01 and ***p<0.001, compared to the
536 control.

537

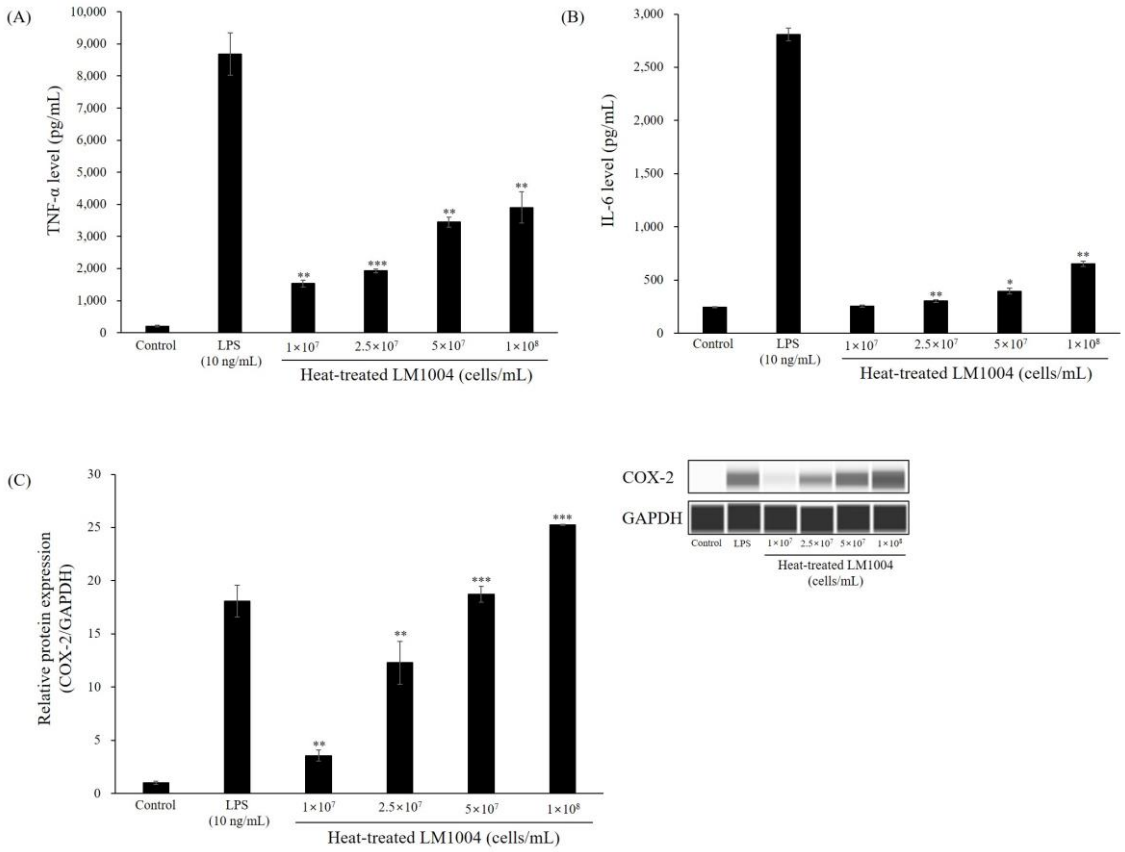

538

539 **Fig. 3. Cytokine production and COX-2 level in heat-treated**
540 ***Lactiplantibacillus plantarum* LM1004 treated RAW 264.7 macrophage cells.**
541 (A and B) concentration of TNF-α and IL-6; (C) COX-2 expression in
542 *Lactiplantibacillus plantarum* LM1004 treated RAW 264.7 macrophage cells.
543 Data are shown as the means±standard deviations of three independent
544 experiments. *p<0.05, **p<0.01, and ***p<0.001, compared to the control.

545

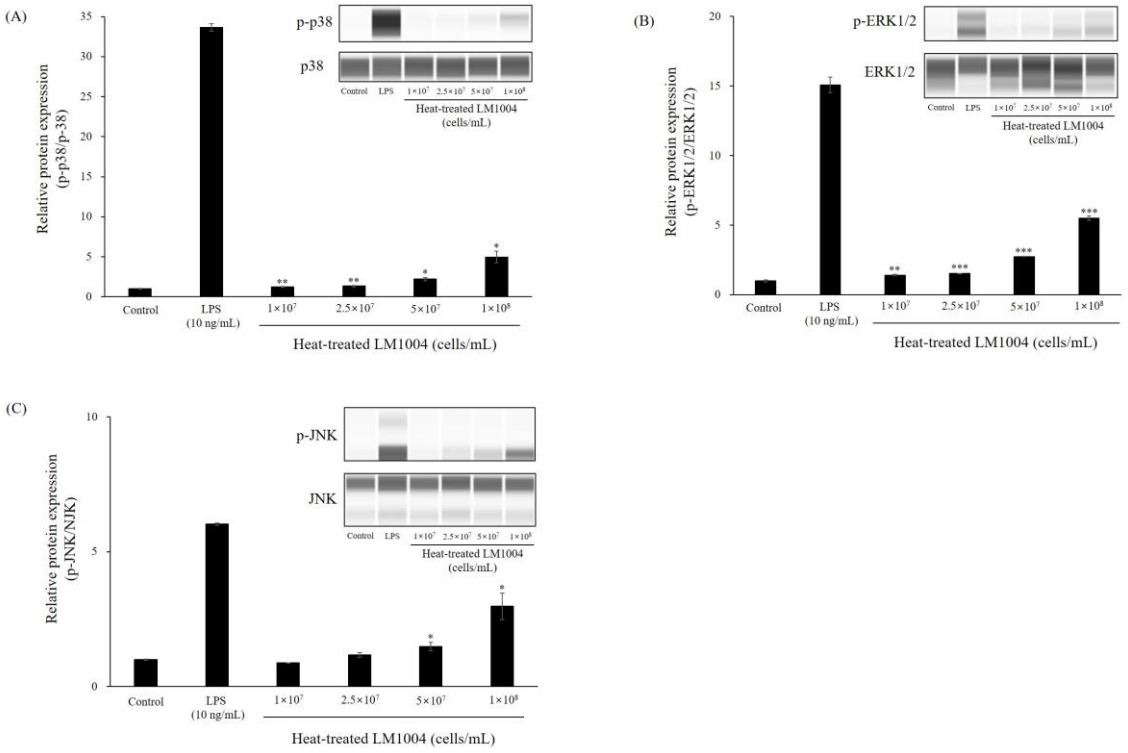

546

547 **Fig. 4. MAPK activation by heat-treated *Lactiplantibacillus plantarum***
548 **LM1004**. Data are shown as the means±standard deviations of three
549 independent experiments. *p<0.05, **p<0.01, and ***p<0.001, compared to the
550 control.

551

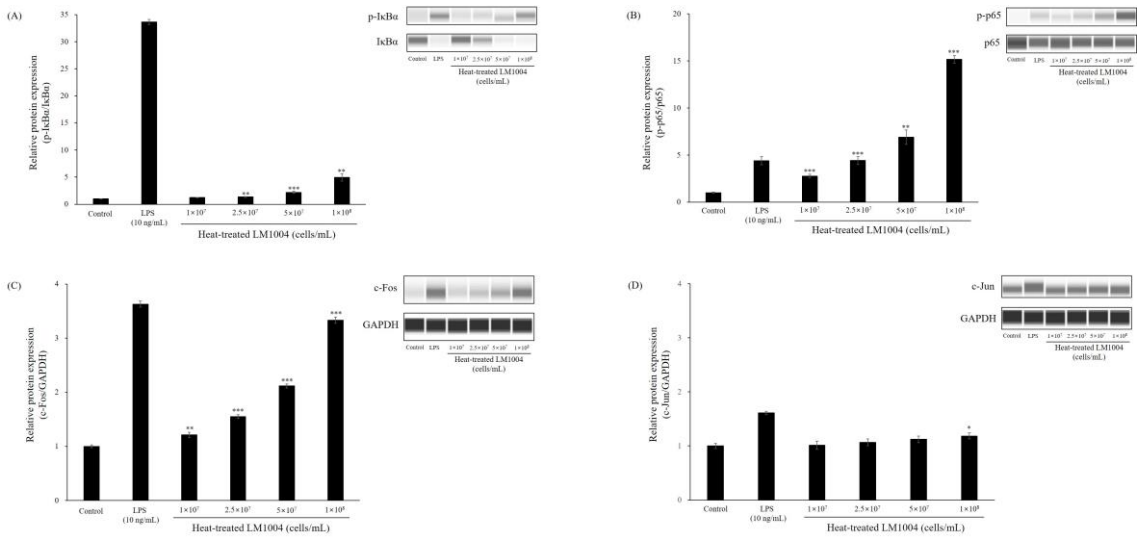

552

553 **Fig. 5. Change of transcription factor protein level in heat-treated**

554 ***Lactiplantibacillus plantarum* LM1004 treated RAW 264.7 macrophage cells.**

555 Data are shown as the means±standard deviations of three independent

556 experiments. *p<0.05, **p<0.01, and ***p<0.001, compared to the control.

557

ACCEPT

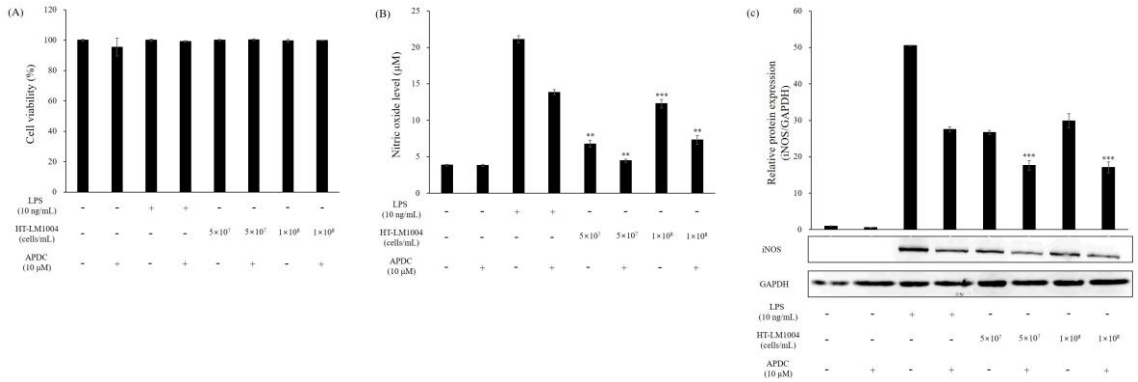

Fig. 6. Modulation of nitric oxide and iNOS protein expression level in ADPC treated RAW 264.7 macrophage cells. ADPC inhibited NF-κB as pharmacological inhibitor. (A) cell viability of RAW 264.7 macrophage cells, (B) production of nitric oxide in NF-κB inhibited cells by heat-treated *Lactiplantibacillus plantarum* LM1004, (C) overexpression of iNOS protein level in NF-κB inhibited cells by heat-treated *Lactiplantibacillus plantarum* LM1004. Data are shown as the means±standard deviations of three independent experiments. **p<0.01 and ***p<0.001, compared to the control (non-treated RAW 264.7 macrophage cells).

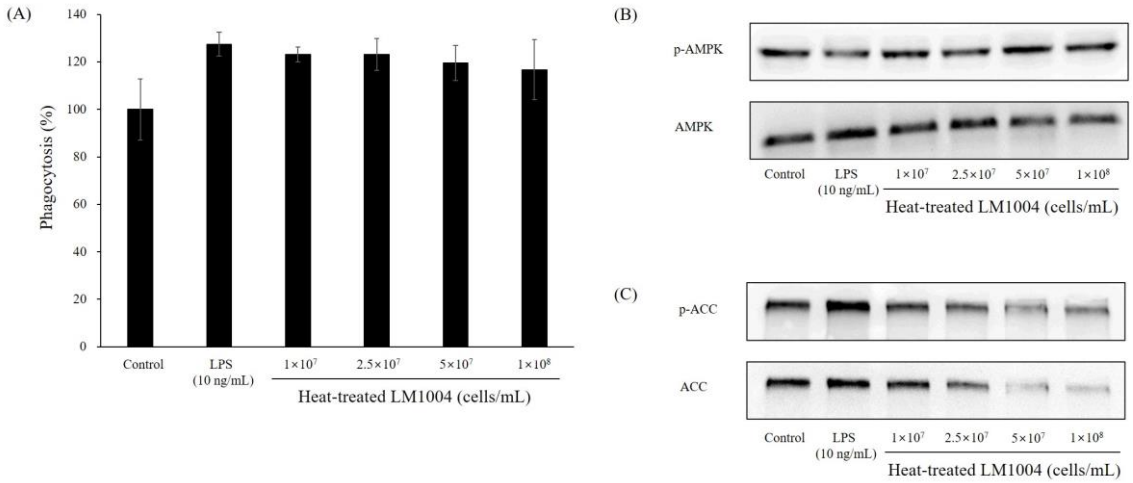

Fig. 7. Phagocytosis of heat-treated *Lactiplantibacillus plantarum* LM1004 treated RAW 264.7 macro-phage cells. (A) phagocytosis effect of heat-treated *Lactiplantibacillus plantarum* LM1004 treated RAW 264.7 macrophage cells, (B and C) AMPK and ACC protein expression level in heat-treated *Lactiplantibacillus plantarum* LM1004 treated RAW 264.7 macrophage cells. Data are shown as the means±standard deviations of three independent experiments.

ACCEPTED